processes

Article

Oil Extraction and Natural Drying Kinetics of the Pulp and Seeds of Commercially Important Oleaginous Fruit from the Rainforests of Guyana

Shaveshwar Deonarine, Navindra Soodoo, Laziz Bouzidi and Suresh S. Narine *

Trent Centre for Biomaterials Research, Departments of Physics & Astronomy and Chemistry, Trent University, 1600 West Bank Drive, Peterborough, ON K9L 0G2, Canada; shaveshwardeonarine@trentu.ca (S.D.); navindrasoodoo@trentu.ca (N.S.); lazizbouzidi@trentu.ca (L.B.)

* Correspondence: sureshnarine@trentu.ca; Tel.: +1-705-748-1011; Fax: +1-705-750-2786

Abstract: Ambient sun drying is the method most used by Indigenous communities for preserving fruits and seeds harvested from the forest. It is an effective method to increase the shelf-life of highly perishable foods and prevent spoilage until important bioactive compounds can be extracted at distant locations. The ambient sun drying kinetics and oil extraction of the pulp and seeds of commercially important oleaginous fruit directly obtained from the rainforests and swamps of Guyana, namely *Astrocaryum vulgare* (Awara), *Astrocaryum aculeatum* (Kuru), *Oenocarpus bacaba* (Turu), *Mauritia flexuosa* (Ite), *Euterpe oleracea* (Acai), *Caryocar nuciferum* (Souari), *Attalea maripa* (Kukrit), and *Carapa guianensis* (Crabwood), were studied. The fruits were dried under ambient conditions from initial moisture contents ranging from 24–71% to a final moisture content of 5%. Three models, the Lewis model, the modified Page model, and the standard logistic function (SLF) model, were utilized to model the drying kinetics and to estimate the parameters governing the drying process. These models were demonstrated to fit the experimental data with excellent goodness of fit (>0.98). The SLF, never used before to model drying kinetics, was observed to be the best-suited model overall, with the highest correlation coefficient and the least Chi-square (χ^2). Depending on the fruit type, the estimated point where the maximum drying rate occurs varies from 35 min to 350 min for sun-dried fruit pulp and up to 4000 min for sun-dried kernels. The steepness of the drying curves varied from −0.5 to −3.5 g/min. The results of this work will aid in the design, development, optimization, and control of the ambient drying processes of economically and functionally important oleaginous forest fruits. This knowledge will assist in addressing the key challenge of spoilage faced by Indigenous communities in the preservation of tropical oleaginous fruits and seeds, possibly aiding in the preservation of functional characteristics of the extracted oils and adducing to the sustainable economic utilization of such fruit.

Keywords: Guyana; Amazonian fruits; *Arecaceae*; *Meliaceae*; *Caryocaraceae*; ambient drying; drying kinetics; oil extraction; mechanical cold-pressing

Citation: Deonarine, S.; Soodoo, N.; Bouzidi, L.; Narine, S.S. Oil Extraction and Natural Drying Kinetics of the Pulp and Seeds of Commercially Important Oleaginous Fruit from the Rainforests of Guyana. *Processes* **2023**, *11*, 3292. https://doi.org/10.3390/pr11123292

Academic Editor: Agnieszka Zgoła-Grześkowiak

Received: 25 October 2023
Revised: 14 November 2023
Accepted: 22 November 2023
Published: 24 November 2023

1. Introduction

The pulp and kernels of fruits from many tropical trees have been shown to have unique sensory, energy, and health characteristics which makes them candidates for significant agribusiness potential [1]. The oleaginous fruit-bearing trees play particularly important ecological roles in the areas where they occur and impact the socio-economic activities of communities where they proliferate. The *Arecaceae* family is the largest, comprising of 198 genera [2] and 3802 species catalogued worldwide [3]. These families are distributed in tropical and subtropical ecosystems and occur over a wide range of latitudes and altitudes. These environments and phylogenetic factors affect their botany and physicochemical characteristics in a complex manner [4–7]. The different characteristics that distinguish them may vary significantly depending on these factors [8]. The variability in the amounts, diversity, and richness of the chemicals stored in the different parts of the plant such as lipids, bioactive components, fibers, proteins, carbohydrates, and minerals indicate great potential in various traditional industries such as foods, pharmaceuticals, and cosmetics as well as large scale applications in emerging bio-industries such as bio-based lubricants and biodiesel [9]. The economic potential of the tropical oleaginous trees in the modern cosmetics and nutraceutical industries is considered notable [10–15]. The fruit in many species is the main part used for human consumption and can be regarded as a functional food due to chemical characteristics that combine nutritional and pharmacological value [16]. They are significant sources of nutritional compounds, including fibers, healthy fatty acids, and bioactive compounds including antioxidants [17]. Agostini-Costa [18] reported that in the use of palm trees for example, the utilization of fruits and seeds accounts for 17–53% and 10–16.5%, respectively, and their oils and fats account for ~33% of the total mass of the tree.

All the parts of the *Arecaceae* palms are traditionally used and these usages are progressively scientifically introduced as part of sustainable local economies. The fruit pulp, oil, fiber, leaves, petioles, sap, palm heart, seeds, and roots are used for construction, food, crafts, rituals, cultural activities, medicines, and household utensils [19]. The species of the *Meliaceae* family, particularly *Carapa guianensis* (Crabwood), is well known and recognized for its oil with reported biological activities including anti-fungal, anti-malarial, anti-inflammatory, insect repelling, and skin protection activities [20–22]. Oils produced from the nuts of plants belonging to the *Caryocaraceae* family are known to have antioxidant, anti-aging, anti-proliferative, and anti-immunomodulatory properties [22].

The *Meliaceae* family is composed of 575 species which are categorized into 50 genera. This family is known to encompass a wide range of plants with known medicinal properties [5]. The *Carapa guianensis* (Crabwood) tree is a prominent species of this family. Extracts from various parts of this tree have been traditionally utilized by indigenous people as a natural remedy for treating wounds, fungal infections, fever, and malaria [23] and as an insect repellent [24]. Crabwood oil is also used in the pharmaceutical and cosmetic industries in products such as soaps, shampoos, and creams [20].

The *Caryocaraceae* family consists of 23 species categorized into 2 genera [6]. The trees of the family are mainly logged and used in construction. The leaves of the plants are traditionally used as a remedy for treating colds and coughs [25]. The seeds are a nutritious source of fiber, proteins, carbohydrates, and minerals. *Caryocar nuciferum* kernel (souari) is considered an exotic super fruit [26]. The souari kernels are soft, sweet, and taste like almonds [27]. The fresh kernel of the species is reported to have high oil yields. The yield reported for Caryocar nuciferum kernel (souari), for example, is 45 w/w% [27]. The kernel oil of the species of the Caryocaraceae family, such as *Caryocar brasiliense*, (pequi) and *Caryocar villosum*, is widely used by indigenous people for cooking, as a butter substitute, and as an effective healing balm [28–31]. It is also an excellent emollient used in the formulation of cosmetic products and soaps [32].

As a result of their high moisture content (>50 w/w%), fresh fruits and seeds of tropical trees are highly perishable, resulting in post-harvest qualitative and quantitative losses if not properly processed and stored. Low moisture contents, typically below 10 w/w%, are required to minimize undesirable changes in nutritional and chemical composition, weight, color, texture, and aroma [33]. By removing moisture from the fresh tropical fruits, drying inhibits bacterial growth and enzymatic activity, thus increasing the product's shelf-life [34].

The drying process can be carried out using natural drying or artificially enhanced drying methods [35,36]. Typically, moisture removal follows three stages. A fourth short warmup period is observed before the water begins to evaporate when a cold material is used. Firstly, water is removed from the saturated surface at a high constant rate. After the surface water is depleted, moisture diffuses slowly to the surface and is lost at a significantly reduced rate. During this falling rate stage, the texture of the material may change and slow diffusion as well. When there is no longer enough evaporation to keep the temperature down, the material tends to heat up and evaporation may take place below the material's surface if there are cracks or pores. This is the second and final falling-rate stage of the drying process [37].

Natural drying consists of exposing whole or sliced fresh fruits and seeds to ambient environmental conditions (in the sun or shade) whereas artificial drying processes use specialized dryers in which drying parameters such as air flux, temperature, humidity, and time are carefully controlled and optimized independently of weather conditions [36,38–40]. Dryers and related drying methods are developed to ensure consistent shelf-life, food safety, and quality on commercial scales. However, these methods usually require larger investment, advanced energy sources, and technical skills to operate and thus can be unaffordable to local communities in hinterland, lowlands, and forest areas.

Although natural drying methods have inherent disadvantages such as dependency on weather conditions, low operational performance, and potential contamination concerns, they are simple, chemical free, and require no modern energy source, complex equipment, or specialized skills. Natural drying is sustainable and considered generally safe if properly handled. This type of drying is suited for areas that do not have modern infrastructure and technologies or facile sources of energy such as local communities in the Amazon and the hinterland in Guyana. These communities have historically taken advantage of direct solar energy to dry tropical fruits. The practice has cultural significance and contributes to the preservation of traditional heritage. Nowadays, foods that are naturally dried are considered high value products and appreciated for their nutrients and flavors as well as sustainable origin [1].

Several studies were conducted on the drying processes and drying kinetics of oleaginous fruits which are the focus of this study using artificial dryers; but no studies are available on natural drying methods at ambient environmental conditions. *Astrocaryum aculeatum* pulp and kernel were dried in a convective fixed bed dryer at different temperatures (50, 60, 70, and 98 °C) and drying kinetics were studied using thin-layer models and fitted with Page, Newton, and Henderson models [41]. Cast-tape drying, freeze drying [42], and Pratic drying with controlled air speed (1.8 ms^{-1}) [43] were also used to dry *Astrocaryum aculeatum* pulp and kernel. Infrared freeze dryers [44], conductive thin-film dryers [45], and laboratory-scale tunnel dryers [46,47] were used to dry *Euterpe oleracea* at controlled temperatures ranging from ~32 °C to 65 °C. *Mauritia flexuosa* pulp were dried milled and dried to produce flour but the drying kinetics study was not performed [48].

Modeling of fruit and vegetable drying has developed significantly from the relatively simple empirical functions to advanced simulations using machine leaning techniques and artificial intelligence [49]. Thin-layer models are among the first approaches to be used to describe the evolution of food moisture content during drying. Since these approaches do not require extensive computation powers to be implemented and provide significant practical insights into drying processes, they are still extensively applied to food drying experimental data.

Thin layer modeling approaches are diverse, including exponential and power functions and more complex functions based on statistics and laws of heat, mass, and momentum transfer. Thin-layer drying models are classified in three categories: empirical, semi empirical, and theoretical [49,50]. Some models, such as the Lewis model, are straightforward but not flexible enough to adapt to the variability in experimental drying and therefore can be applied to describe only limited drying data sets. The models with insignificant and correlated parameters and those which require a transformation of the data, while generally fitting experimental data well, fail to provide meaningful insights into the physics of the drying process and are therefore to be avoided. The thin layer drying functions suggested by Buzrul [51] to model and describe the existing drying data of fruits and vegetables can be narrowed down to two classes of models that yield similar results as follows:

1. Logarithmic class: this class includes the Lewis (Newtonian) model [52] and the so-called modified two-term model [53,54];

2. Sigmoidal class: this class includes the Page model [55], the modified Page model [56], and the Weibull model [57,58].

In the logarithmic and sigmoidal classes the scale parameter (t_0) indicates the time needed to accomplish a given amount of moisture. t_0 is a characteristic time specific to each model. For example, t_0 of the Weibull model represents the time needed to achieve approximately 63% of the process. The exponent, *(n)*, is known as the shape parameter and indicates the growth rate and steepness of the curve. In cases where mass is used instead of moisture ratio (MR), as is the case in this work, content in the modeling, initial mass (maximum), and dynamic equilibrium mass (minimum) are introduced in the forms and may be constrained or not during regression, depending on predetermined conditions. The correlation of fit parameters is an estimation of the independence of these parameters. It is an important statistical tool used to assess a model's validity to describe experimental data. It is generally indicated by the following qualifiers: strong, mild, or low [59].

The natural drying process is subjected to fluctuation in environmental conditions which results in complex drying kinetics and drying curves that do not lend themselves easily to modeling as those obtained in the more controlled processes such as in oven dryers [60]. Understanding and quantifying factors affecting ambient drying in relation to characteristics of the dried material, equipment design, and environmental conditions would help in the design, development, optimization, and control of local fruits and seeds' drying processes [36].

This work evaluates the oil extracted by a mechanical cold press from the pulp and/or kernel of eight commercially important oleaginous fruit directly obtained from the rainforests and swamps of Guyana: *Astrocaryum vulgare* (AV, Awara), *Astrocaryum aculeatum* (AA, Kuru), *Oenocarpus bacaba* (OB, Turu), *Mauritia flexuosa* (MF, Ite), *Attalea maripa* (AM, Kukrit) *Euterpe oleracea* (EO, Acai) *Caryocar nuciferum* (CN, Souari), and *Carapa guianensis* (CG, Crabwood). The work also describes ambient drying of AV, AA, OB, EO, and MF pulp and AV, AA, CG, and CN seeds. The drying kinetics of these fruit pulps and seeds were described using three selected models: the Lewis model, the modified Page model, and a generalized logistic function known as the standard logistic model. To the best of our knowledge, there are no published modeling studies of natural/solar drying kinetics of tropical fruits.

2. Materials and Methods

2.1. Materials

For conciseness and easy reading, acronyms using the initial letters of the scientific name of the species followed by the initial letter of the nature of the fruit material (pulp (P), seed (S), and kernel (K)) were used to name the different materials of this study.

Fruit Species, Collection, and Processing

The eight different fruits and seeds of the oleaginous tree species studied in this work were sourced from Indigenous communities across three regions of Guyana, South America. The fruits do not grow in the same regions due to important geographical and environmental differences. Figure 1 presents the administrative and natural regions of Guyana from which the fresh fruits and seeds were sourced. Fresh fruits of AA, OB, MF, CG, and AM were supplied by the indigenous residents of Region #1 (Hinterland Forest, yellow star in Figure 1). AV fruits were supplied by residents of Region #2 (coastal plains, red star in Figure 1). EO and CN were supplied by residents of Region #9 (Rupununi Savannahs, blue star in Figure 1).

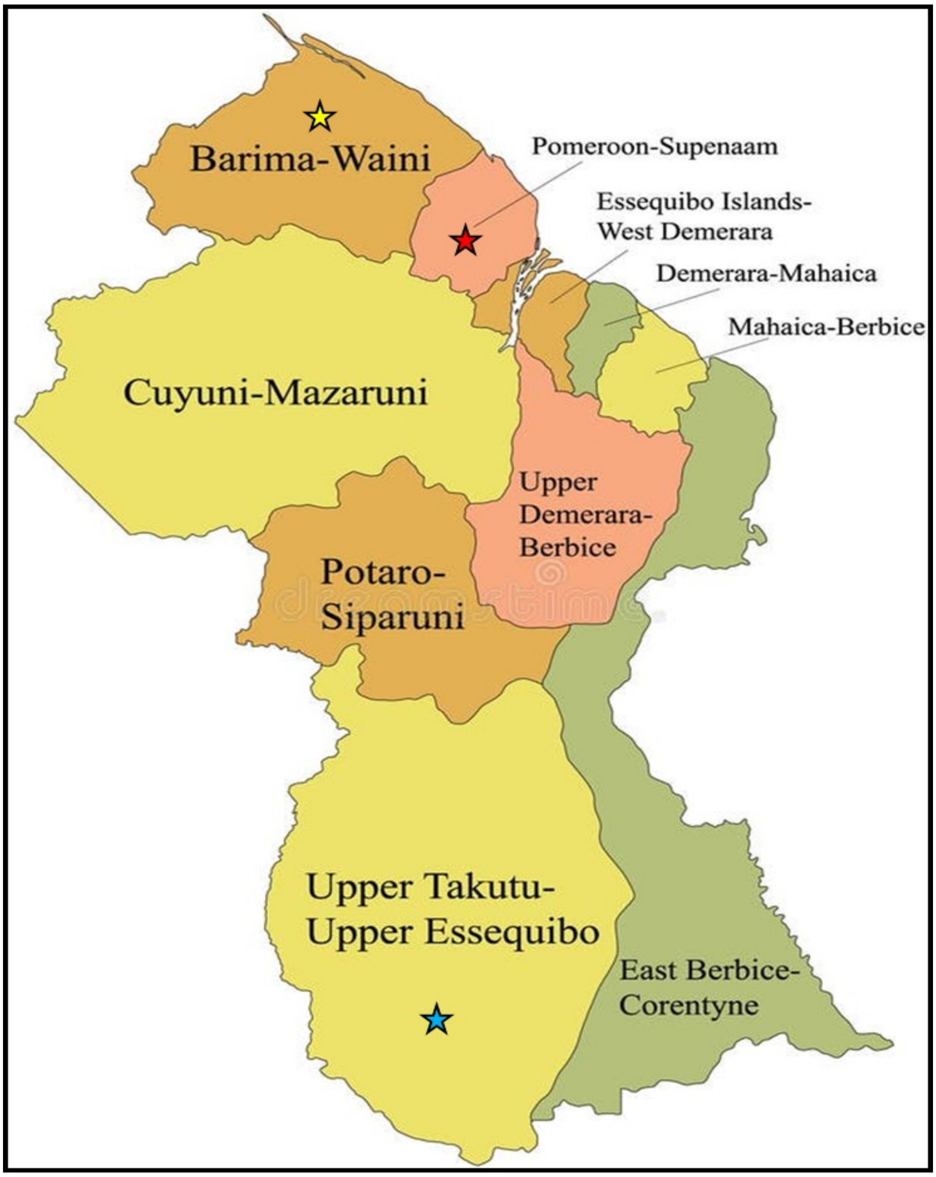

Figure 1. Regions of Guyana outlining where the fresh fruits and seeds were sourced. Inset is a map of the natural regions. *Astrocaryum aculeatum* (AA), *Oenocarpus bacaba* (OB), *Mauritia flexuosa* (MF), *Carapa guianensis* (CG), and *Attalea maripa* (AM) from Region #1 (yellow star); *Astrocaryum vulgare* (AV) from Region# 2 (red star); and *Euterpe oleracea* (EO) and *Caryocar nuciferum* (CN) from region 9 (blue star). Image source: https://www.dreamstime.com/map-administrative-division-guyana/ (accessed on 1 October 2023).

To maintain the integrity of the samples and prevent spoilage, each fruit was individually inspected. Fruits that were unripe or demonstrated bruises, blemishes, or signs of microbial deterioration were excluded from the experiments. All stems, twigs, and leaves attached to the fruits were manually removed using stainless steel knives and then washed with distilled water.

AV, AA, OB, EO, MF, and AM have a firm fibrous pulp surrounding the rigid seed. The pulps were separated from the seed using stainless steel knives/vegetable peelers. The seeds of AV, AA, CN, and CG were split using a knife and hammer to expose the kernels.

2.2. Methods

2.2.1. Drying Setup

Out of the 18 materials listed in Table 1, the following seven (7) materials: *Astrocaryum vulgare* pulp (AVP), *Astrocaryum aculeatum* seed and kernel (AAP and AAS), *Oenocarpus bacaba* pulp (OBP), *Euterpe oleracea* pulp (EOP), *Mauritia flexuosa* pulp (MFP), and *Carapa guianensis* seed (CGS) were selected for drying kinetics studies as they are representative of the pulps and seeds collected for this study.

Table 1. Acronyms for fruit, fruit pulp, fruit seed, and/or fruit kernel investigated in this study.

Scientific Name	Fruit Acronym	Fruit Material	Material Acronym
Astrocaryum vulgare	AV	Pulp	AVP
		Seed	AVS
		Kernel	AVK
Astrocaryum aculeatum	AA	Pulp	AAP
		Seed	AAS
		Kernel	AAK
Oenocarpus bacaba	OB	Pulp	OBP
		Seed	OBS
Euterpe oleracea	EO	Pulp	EOP
		Seed	EOS
Mauritia flexuosa	MF	Pulp	MFP
		Seed	MFS
Attalea maripa	AM	Seed	AMS
		Kernel	AMK
Carapa guianensis	CG	Seed	CGS
		Kernel	CGK
Caryocar nuciferum	CN	Seed	CNS
		Kernel	CNK

Although drying kinetics were not performed on the other materials, kernels of AVK, AAK, AMK, CGK, and CNK were dried and oil was extracted from these materials using the cold press expeller.

The drying kinetics of fresh pulps and seeds were performed in triplicate using a rectangular aluminum pan (Length × Width × depth of 26 cm × 20 cm × 6 cm). A known mass of evenly chipped fruit pulp (3–4 cm long, 0.5–1 cm thickness) was evenly spread in a thin layer (0.5–1 cm thick) into the aluminum pan in a similar manner to conventional thin layer drying setups [61]. Split fruit seeds were similarly arranged in a single layer into the pan but with all the kernels facing upwards for direct exposure to the sun. For sun-dried kinetics studies, the drying pans were directly placed into sunlight. For drying kinetics experiments conducted in the shade, samples were placed outdoors under a shed to avoid exposing the fruit to direct sunlight. All sun-dried and shade-dried experiments were performed in ambient environmental conditions. The shade drying experiments were carried out to describe drying under intermittent sunlight which frequently occurs in Guyana. The method was discontinued because it resulted in spoilage during the experiment. The sample weight loss and temperature were measured every 30 min using a digital mass balance (Kalorik®, Miramar, FL, USA) and Fluke 568 infrared thermometer (ITM Instruments, York, ON, Canada) until three constant weight loss values were measured. The relative humidity was obtained from meteorological records using weather.com (accessed on 15 July 2023) and was not measured on site [62].

2.2.2. Moisture Content and Pulverization

The moisture content of the materials was recorded before the start of the drying experiment (fresh pulp/seed) and at the end of the drying experiment (when three constant mass values are measured) using an MB45 moisture analyzer (OHAUS, Moris County, NJ, USA) at 100 °C. The materials were then pulverized using a high speed multifunctional comminutor (Seeutek®, CA, USA) and stored in sealed bags (Ziploc®, SC Johnson, Brantford, ON, Canada) for oil extraction.

2.2.3. Oil Extraction and Mass Balance

Pulp and seed oils were extracted from the dried/pulverized samples using a 1500-Watt portable cold press oil expeller (CGOLDENWALL, Beijing, China). Pulp oil of AV, AA, OB, EO, and MF were extracted between 30 °C and 40 °C. Seed oil of AV, AA, CG, and CN are solid at room temperature and were extracted between 50 °C and 80 °C to melt the oil so it can be expelled. Oil from the seeds of OB, EO, and MF could not be extracted using this method because the kernels were attached to the hard fibrous shell in a way that prevented proper separation and pulverization. The materials obtained from the seeds of these fruits clogged the expeller at the feeding stage, preventing oil extraction.

The pulverized samples were fed through the expeller twice to increase the oil yield. All expelled oil was vacuum filtered using Coarse Whatman #40 filter paper to remove the insoluble particles from the oil. The oils were then stored in glass bottles.

A mass balance study was performed for each fruit batch studied. The mass balance data accounts for the mass of fresh fruit, fresh pulp, dried pulp, pulp oil, fresh kernel, dried kernel, deshelled kernel, kernel oil, pulp flour, kernel flour, and filter paper residue. The mass balance results are reported in Section 3.3.

2.2.4. Mathematical Modeling of Drying Kinetics

Curve fitting of the mass versus time data collected during ambient drying of AAP, AAS, AVP, EOP, OBP, MFP, and CGS was performed using a representative function of each of the two model classes identified in Table 2, namely the Lewis ((i) in Table 2) and the modified Page ((iv) in Table 2) models. The Lewis model proposes that change in moisture content during the falling-rate stage is proportional to the moisture difference to the equilibrium state under the drying conditions [63]. The modified Page model is derived based on an approximated solution of Fick's law of diffusion and has generally been shown to provide good fits to experimental data where the falling-rate stage is the main drying stage [64]. In addition to the above two models, a special case of the generalized logistic function (Richards's curve) known as the standard logistic function (SLF), was used to model the experimental data. The generalized logistic function is suitable for this purpose because it allows for more flexible S-shaped curves without increasing the number of parameters or altering their significance [65]. It is an extension of the original logistic or sigmoid functions which were developed to model population dynamics and more general biological growth under probabilistic assumptions [65]. It is applied for the prediction of a variety of growth phenomena such as tumors [66], the concentration of reactants and products [67], and epidemic trends such as COVID 19 [68].

SLF generates an *S*-shaped curve which has four significant parameters:

$$y = min + \frac{max - min}{(1 + (\frac{t}{t_0})^{-n})} \tag{1}$$

where min and max are two asymptotes parallel to the t-axis which indicate the minimum and maximum of the curve, respectively. At t = 0, $y(0) = max$, which in our case is the starting mass of the material, and at $t = \infty$, $y(\infty) = min$, which in our case is the dynamic equilibrium that mass reaches in ambient drying. t_0 is the scale parameter of the function. It is a characteristic time at which the curve has an inflection point and the curve slope is maximum. n is the shape parameter of the function. It indicates the growth rate or steepness (hill slope) of the curve. The shape parameter is an expression of various mechanisms involved in the drying process and is related to the speed of mass transfer at the start of the falling rate stage [69].

Table 2. Classes of suggested thin-layer drying models.

Class		Model Name		Parameter Correlation	Comment	Ref
Logarithmic	(i)	Lewis (Newton)	$MR = e^{-\frac{t}{t_0}}$		Simplest but fails to model many drying data	[52]
	(ii)	Modified two-term	$MR = ae^{-\frac{t}{t_0}} + (1-a)e^{-b\frac{t}{t_0}}$	Mild to strong		[53,54]
Sigmoidal	(iii)	Page	$MR = e^{-\frac{t}{t_0}^{n}}$	Strong	Simple, describes many drying data	[55]
	(iv)	Modified Page	$MR = e^{-\left(\frac{t}{t_0}\right)^n}$	Low	Same as Page model with fewer errors on the rate parameter	[56]
	(v)	Weibull	$MR = e^{-\left(\frac{t}{t_0}\right)^n}$	Low	Simple, describes many drying data	[57]
			$MR = 10^{-\left(\frac{t}{t_0}\right)^n}$	Mild	Simple, describes many drying data.	[58]
	(vi)	Standard Logistic Function	$MR = min + \frac{max-min}{\left(1+\left(\frac{t}{t_0}\right)^{-n}\right)}$	Mild	Can describe many experimental data	This work

Similar to the arguments invoked for the Weibull probabilistic approach to mass change during drying [70], the SLF considers that the mass change from an initial value (max) to a final dynamic equilibrium value (min) is represented under the specified experimental conditions by a continuous random variable with a sigmoid probability density function. The SLF parameters are weakly correlated like those of the Weibull model. Unlike in the other models, the characteristic time of the SLF, t_0, and exponent, n, are interpretable parameters easily identified by visual inspection of the data. The versatility and potential of SLF to describe the processes of varied experimental drying data sets were examined and compared with those of the widely used Lewis and modified Page thin layer model.

Drying rate (DR), defined as the loss of mass from the wet solid per unit of time (t), was calculated from the curves generated by the fit to the drying data using the models according to

$$DR = \frac{dM(t)}{dt} \tag{2}$$

Built-in and user-defined equations in the nonlinear regression wizard of Sigmaplot 12.5 software were used to fit the data. Since modeling the average values with the error bars for independent replicates is considered a lesser choice [71,72], all replicates were individually modeled and the results were analyzed statistically as recommended [71].

2.2.5. Statistical Analysis

Statistical evaluation of the results was performed using a design including the three models (Lewis, modified Page, and SLF); ambient drying experiments of the pulps and seeds of AAP, AAS, AVP, EOP, OBP, MFP, and CGS were each performed in triplicate. The coefficient of determination (R^2), Chi-square (χ^2), and residual sum of squares (RSS) were used to evaluate the performance of the models. A Shapiro–Wilk test and coefficient of concordance (W Statistic) were used to assess normality and agreement. The Durbin–Watson (DW) statistic was used to test for autocorrelation in the residuals. Standard error and standard deviation were used to assess the physical relevance of the models' parameters. Residuals and analysis of variance (ANOVA) were conducted to compare the experimental and predicted values between the fitted curves. The statistical analysis was performed using the Sigmastat module of Sigmaplot 12.5 software.

3. Results and Discussion

3.1. Drying Kinetics and Modeling of the Experimental Data

The experimental mass versus drying time data obtained in this work are provided in the Supplementary Materials in Table S1. The mass changes of the samples, which indicate moisture content changes [73], were used for the regressions because no other mass loss occurred during the experiments. The relevant data were converted to moisture content considering the measured initial moisture. The curves resulting from the application of Lewis, modified Page, and standard logistic models, represented by Equations (i) and (iv) of Table 2 and Equation (2), to the experimental data are provided in Figure S1. The fit parameters and related statistical data for the three models are presented in Table 3. The data for the minimum values obtained from the fits and presented in Table 3 were normalized using the fixed maximum mass at 100. Figure 2 shows the predicted curves obtained with the standard logistic model on observed mass loss data for fresh sun-dried and sun-dried seeds.

Table 3. Drying kinetics data. (a) Sun-dried pulp, (b) sun-dried seeds. M. Page: Modified page model; SLF: Standard logistic function; Lewis: Lewis model.

(a) Sun-Dried Pulp									
	AAP			**AVP**			**EOP**		
	SLF	**M. Page**	**Lewis**	**SLF**	**M. Page**	**Lewis**	**SLF**	**M. Page**	**Lewis**
χ^2	0.373	0.445	0.385	0.211	1.3851	1.56	0.150	0.089	0.215
R^2	0.996	0.991	0.987	0.988	0.994	0.986	0.996	0.998	0.994
RSS	56.7 ± 12.6	49.2 ± 12.0	88.2 ± 36.8	335.4 ± 320.3	60.6 ± 12.2	196.5 ± 47.6	21.4 ± 4.9	11.0 ± 0.6	33.1 ± 8.7
t_0 (min)	283.3 ± 59.9	260.7 ± 30.8	347.1 ± 22.1	201.6 ± 15.1	222.5 ± 7.9	288.6 ± 26.6	76.5 ± 1.2	95.1 ± 1.2	98.5 ± 2.4
n	1.3 ± 0.2	1.2 ± 0.1	1.0	0.9 ± 0.1	1.2 ± 0.2	1.0	1.7 ± 0.1	0.95 ± 0.1	1.0
min (%)	63.1± 9.7	47.8 ± 4.7	39.3 ± 1.4	56.5 ± 0.2	35.2 ± 9.4	45.7 ± 1.4	61.7 ± 0.3	61.8 ± 0.3	63.3 ± 0.6

	OBP			**MFP**		
	SLF	**M. Page**	**Lewis**	**SLF**	**M. Page**	**Lewis**
χ^2	0.362	0.514	0.5888	2.23	1.277	2.587
R^2	0.992	0.9916	0.989	0.991	0.993	0.99
RSS	41.8 ± 19.7	65.1 ± 33.1	58.6 ± 34.2	513.3 ± 106.5	408.4 ± 100.5	573.4 ± 103.9
t_0 (min)	66.1 ± 2.1	91.4 ± 3.2	91.4 ± 2.3	454.4 ± 25.1	470.5 ± 22.5	586.5 ± 74.7
n	1.3 ± 0.1	0.9 ± 0	1	1.5 ± 0.1	1.4 ± 0.1	1
min (%)	44.6 ± 30.7	64.8 ± 0.5	65.9 ± 1.3	61.7 ± 0.3	25.7 ± 0.4	13.1 ± 2.41

(b) Sun-dried seeds						
	AAS			**CGS**		
	SLF	**M. Page**	**Lewis**	**SLF**	**M. Page**	**Lewis**
χ^2	0.659	0.793	0.859	0.151	0.151	0.211
R^2	0.995	0.994	0.99	0.991	0.991	0.989
RSS	93 ± 47.8	24,968.6 ± 42,209.4	672.5 ± 977.5	94.7 ± 27.4	94.7 ± 27.9	119.0 ± 43.9
t_0 (min)	475.5 ± 191.1	359.3 ± 56.13	395.3 ± 56.6	2315.5 ± 1520.5	1361.6 ± 755.7	535.6 ± 20.9
n	1.3 ± 0	1.242 ± 0.249	1	0.8 ± 0.1	0.8 ± 0.1	1
min (%)	67.3 ± 5.3	70.7 ± 3.7	69.1 ± 2.7	50.6 ± 15.3	66.1 ± 8.8	78.4 ± 0.7

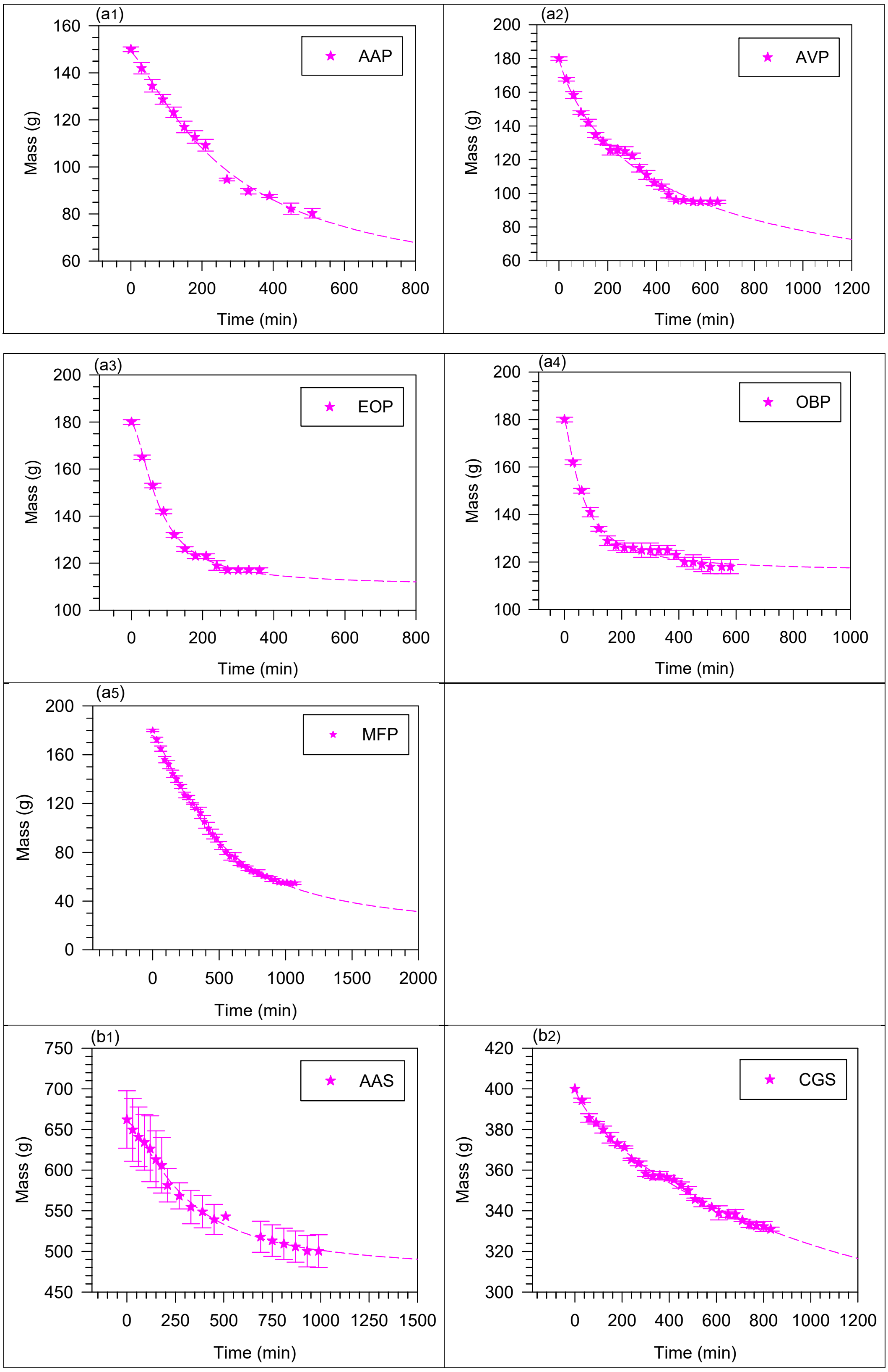

Figure 2. Observed mass loss data as a function of time predicted by the standard logistic model for fresh sun-dried pulps of (**a1**) *Astrocaryum aculeatum* (AAP), (**a2**) *Astrocaryum vulgare* (AVP), (**a3**) *Euterpe oleracea* (EOP), (**a4**) *Oenocarpus bacaba* (OBP) and (**a5**) *Mauritia flexuosa* (MFP) and sun-dried seeds of (**b1**) *Astrocaryum aleatum* (AAS) and (**b2**) *Carap guianensis* (CGS).

3.1.1. Goodness of Fit

The coefficient of determination (R^2), Chi-squared (χ^2) test, and residual sum of squares (RSS) were used to determine the goodness of fit of the three models employed and to assess their potential to describe experimental ambient drying data. The coefficient of determination (R^2) values obtained from the three models were higher than 0.9 for all materials, suggesting that these models are suitable to describe the experimental drying data. However, in scenarios characterized by a steep regression surface, the R^2 value is inflated irrespective of the actual goodness of fit achieved [74]. The χ^2 test was used to further assess the goodness of fit and compare the three models. The SLF displayed the lowest χ^2 values for all materials except for the sun-dried pulp of EO (acai) for which the modified page model yielded the lowest value. Comparison of experimental values with predicted mass values by the modified page and SLF models for EO sun-dried pulp is shown in Figure 3 to visually illustrate the differences in the goodness of fit between the two models. As seen in the figure, the correspondence is excellent (fit to a line provided a R^2 = 1 and a slope of 1).

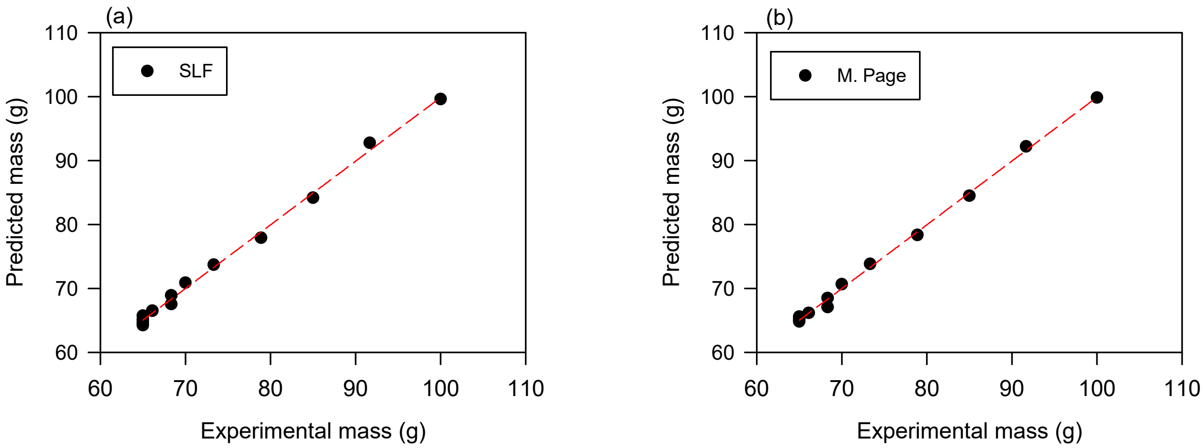

Figure 3. Comparison of experimental with predicted mass for *Euterpe oleracea* sun-dried pulp by (**a**) the modified Page and (**b**) SLF models. Dashed lines are linear fits of the data (R^2 = 1, slope = 1.0 ± 0.02).

Several factors can contribute to the ability of a specific model to describe a given data set including the quality of the data, characteristics of the material, and environmental conditions which can significantly influence the diffusion mechanisms at the different stages of the drying process. A large enough deviation in these factors may skew the drying process enough to no longer be described by a function that otherwise describes similar materials. Although, generally, SLF predicted the experimental ambient drying data with better goodness of fit, the modified Page model may, in specific instances, be more suitable. Regardless, all the statistics indicate that the modified Page is also a model that can very well describe the ambient drying of oleaginous fruits of Guyana. In addition, it lends itself to directly estimating coefficients of diffusion by comparison to approximated solutions of Fick's second law of diffusion. The Lewis model consistently exhibited the highest χ^2 and RSS values for each material and is therefore deemed the least suitable model to represent the drying kinetics of the pulps and seeds in this study.

The agreement of the predictions obtained with the models indicates that the experimental drying patterns in ambient conditions can be unambiguously described with thin-layer approaches. This also indicates that the experimental data are not overfitted, implying that these models, particularly the SLF, can be used to successfully describe the drying kinetics under natural environmental conditions of other similar materials.

3.1.2. Drying Parameters

The dynamic equilibrium values predicted by the models are close to the practical equilibrium determined experimentally. Relative mass loss (%) $ML(\%) = \frac{max-min}{max} \times 100\%$

calculated from the predicted max and min values for the three model compared to measured mass loss is provided in Table 4.

Table 4. Predicted and measured mass loss (%). SLF: Standard logistic function, M. Page: Modified page model, Lewis: Lewis model.

Materials	Mass Loss (%)			
	Experimental	**SLF**	**M. Page**	**Lewis**
		Sun dried pulps		
AAP	46.5 ± 0.8	63.1 ± 9.7	49.6 ± 9.4	60.7 ± 1.4
AVP	47.0 ± 0.6	43.5 ± 0.2	68.0 ± 9.4	54.3 ± 1.4
EOP	35.0 ± 0.6	38.0 ± 0.3	35.1 ± 0.3	36.7 ± 0.6
MFP	69.6 ± 0.6	90.6 ± 0.7	74.5 ± 0.4	86.9 ± 4.9
OBP	34 ± 1.0	36.6 ± 1.7	34.4 ± 1.5	34.1 ± 1.3
		Sun-dried seeds		
AAS	24.1 ± 3.1	29.4 ± 2.3	26.2 ± 1.9	26.6 ± 2.7
CGS	17 ± 0.1	61.5 ± 6.2	38.1 ± 8.7	38.1 ± 8.1

The three models predicted ML(%) in good coincidence with most measured moisture loss (Table 4). The three models predicted ML(%) for EOP, OBP, AAP, and AAS with similar goodness of fit. SLF provided the best ML(%) predictions for sun-dried AVP, EOP, and OBP. SLF provided the best ML(%) predictions for sun-dried AVP, EOP, and OBP. It preditcted higher ML(%) than what was experimentally measured for sun-dried pulps of AAP and MFP and seeds of AAS, suggesting that ambient drying of these materials did not achieve dynamic equilibrium and that they can be further dried to lower moisture content. The modified Page model predicted an ML(%) that is not statistically different from the experimental measurements for sun-dried AVP, EOP, OBP, and sun-dried AAS. M. Page performance is particularly notable for sun-dried AAP as substantiated by its lowest Chi-squared statistics.

The standard logistic and modified Page models provided values of the shape (n) and scale (t_0) parameters which are not significantly different ($p < 0.05$) for the drying kinetics of each material. The shape parameter (n) ranged from 0.6 to 1.71, similar to what is reported for the drying kinetics of other fruits and herbs [75–80]. The shape parameter is an expression of various mechanisms involved in the drying process including diffusion, convection, and relaxation and is related to the pace of mass transfer at the start of the falling rate stage. Lower n values are indicative of faster drying rates. When $n = 1$, the distribution reduces to first order kinetics [57].

Values of the scale parameter t_0 for the sun-dried pulps depended on the species. As shown in Figure 4, t_0 of sun-dried pulps increases from ~66 min for OBP and EOP to ~466 min for MFP, indicating very different diffusion processes in these fruits explained by completely different textures and initial moisture content. This parameter characterizes the different fruits depending on internal structure, moisture content, and effective transport parameters. One direct observation is that higher n values are related to more intricate textures. The n value of EOP, which is the most fibrous and has the most intricate texture, is the highest ($n = 1.7$) followed by that of the less fibrous MFP ($n = 1.5$) compared to AAP ($n = 1.3$) and AVP ($n = 0.9$), which have less and softer fibers, as indicated by easy mastication.

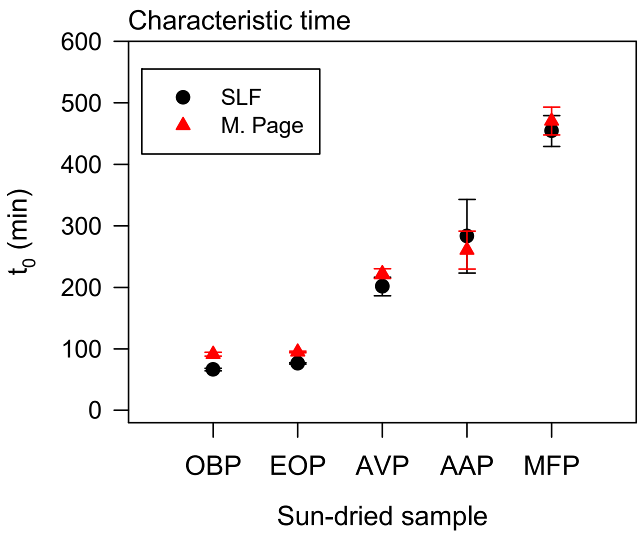

Figure 4. Scale parameter t_0 for sun-dried pulp of fruits obtained with the modified Page (M. Page) and standard logistic models (SLF).

These results indicate that the proposed models are suitable for predicting the moisture content of Guyana's oleaginous fruits (pulp and seed) during drying at local ambient temperatures and can be utilized to estimate important parameters of the drying process. These parameters are suitable for the optimization of local operational conditions.

3.1.3. Drying Rate

The drying rates, defined as the loss of moisture per unit time ($DR = \frac{dMR}{dt}$) of sun-dried pulp and sun-dried seeds, are shown in Figure 5. The same surface area, 0.052 m^2, was used for all drying experiments.

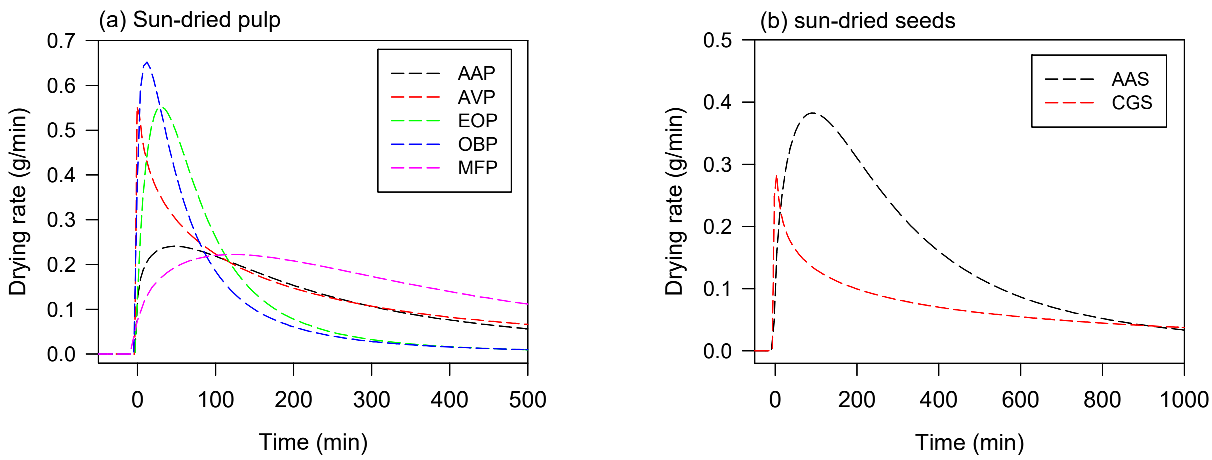

Figure 5. Drying rates of (**a**) sun-dried pulp and (**b**) sun-dried seeds of oleaginous fruits from Guyana.

The shape of the $DR(t)$ curve and its different segments are related to the different stages that the drying process undergoes. As shown in Figure 5, $DR(t)$ curves present maxima (DR_m) at t_s (time at the peak of the drying rate curve) and then generally decrease with time. In the first stage of drying, water is removed from the saturated surface at an increasing rate; then, after surface water is depleted, moisture diffuses slowly to the surface and is lost at a significantly reduced rate. The time at which the surface moisture is depleted is therefore indicated by t_s. The drying stage following surface moisture depletion is known as the falling rate stage. In this stage, the texture of the material may change and slow diffusion as well. When there is no longer enough evaporation to keep the temperature down, the material tends to heat up and evaporation may take place below the material's surface through cracks and pores. Drying in this second and final falling-rate stage of the drying process is slower [37]. The first and second falling-rate stages are represented in the $DR(t)$ curve by two straight segments joined by a bent decaying line indicating the existence of a region where the two stages of drying coexist.

There is no correlation between DR_m or t_s with initial moisture of the sample. This is expected because although it is related to the capacity of the microstructure to hold moisture, the details of microstructure can be quite different from fruit to fruit, making any inference practically impossible with the simple model used to describe the drying process. The slope of the line representing the first falling stage (α_1), although seeming to correlate with the initial moisture content of AAP, EOP, OBP, and AVP, is probably serendipitous as it is also the result of the details of the fruit microstructure. The difference in drying rates can be related to the pressure difference between the sample center and surface wherein higher-pressure differences lead to faster diffusion of moisture from the sample.

3.2. Extraction of Oil from Dried Fruit

Figure 6 shows the fruits at various stages of the drying process and the appearance of the extracted oil as follows: (i) AV, (ii) AA, (iii) OB, (iv) EO, (v) MG, (vi) CG, (vii) CN, and (viii) AM.

3.2.1. Fruit and Oil Description

Table 5 presents information on the characteristic color, shape, size, fruit mass, pulp mass, and kernel mass (excluding shell) for the eight fruits studied.

Table 5. Description of the fresh fruits studied. Data are based on averages on a measurement of 10 fruits.

	Fruit	Fruit Colour	Shape	Length (cm)	Width (cm)	Fruit Mass (g)	Pulp Mass (g)	Kernel Mass (g)
(i)	AV	Orange	Oval-spherical	4.4 ± 0.8	3.2 ± 0.6	31.8 ± 11.3	18.0 ± 7.6	17 ± 3.2
(ii)	AA	Yellow-green	Oval-spherical	5.6 ± 2.3	5.2 ± 1.2	41.1 ± 13	25.9 ± 1.0	21.3 ± 4.6
(iii)	OB	Purple	Elliptical-globular	3.54 ± 0.1	3.04 ± 0.5	11.2 ± 2.4	4.2 ± 0.3	6.66 ± 1.7
(iv)	EO	Purple	Globular	1.4 ± 0.1	1.3 ± 0.1	1.32 ± 0.1	0.42 ± 0.1	0.9 ± 0.1
(v)	MF	Chestnut	Globular-elongated	5.75 ± 0.4	4.70 ± 0.5	55.1 ± 9.8	18.7 ± 3.3	20.83 ± 7.4
(vi)	CG	Yellow-brown	Irregular quadrilateral	7.1 ± 0.4	5.8 ± 0.1	19.6 ± 4.4	-	14.8 ± 1.5
(vii)	CN	Yellow-brown	Kidney-shaped	7.46 ± 0.2	6.56 ± 0.2	123.6 ± 10.5	-	23 ± 3.8
(viii)	AM	Cream-yellow	Oblong ovoid	4.9 ± 0.2	2.3 ± 0.1	20.3 ± 1.5	4.7 ± 1.4	9.8 ± 0.6

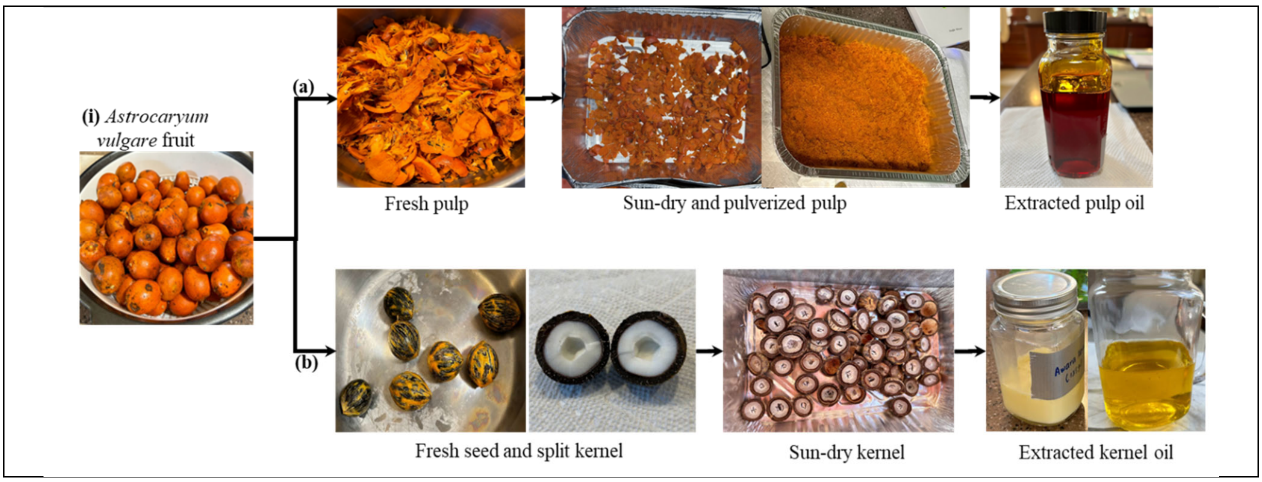

Figure 6. *Cont.*

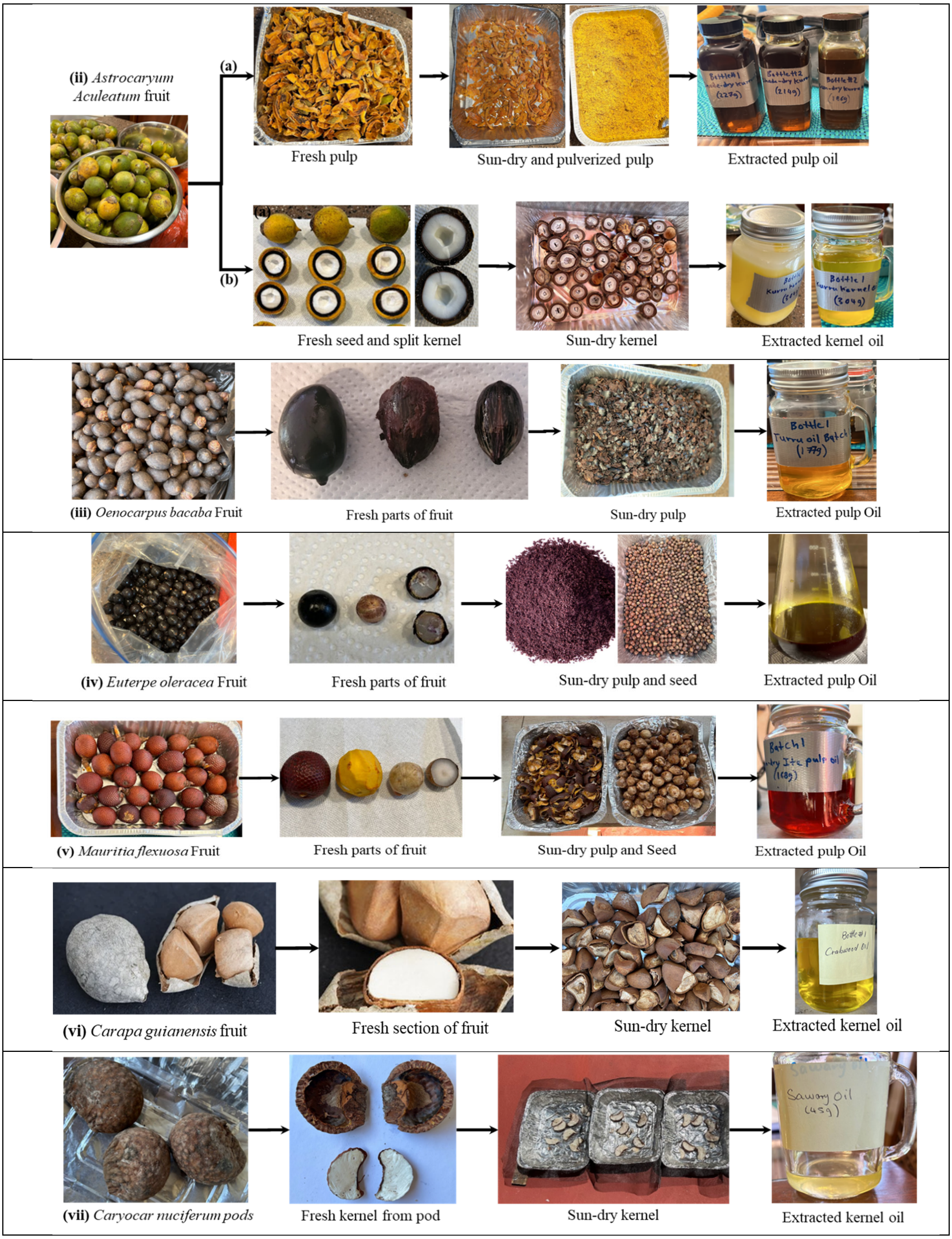

Figure 6. *Cont.*

Figure 6. Pictograph of the drying process and extraction of oil from the pulp and kernels (**i**) *Astrocaryum vulgare* (AV) (**i-a**) pulp (**i-b**) kernel, (**ii**) *Astrocaryum aculeatum* (AA) (**ii-a**) pulp (**ii-b**) kernel, (**iii**) *Oenocarpus bacaba* (OB), (**iv**) *Euterpe oleracea* (EO), (**v**) *Mauritia flexuosa* (MF), (**vi**) *Carapa guianensis*, (CG) (**vii**) *Caryocar nuciferum* (CN), and (**viii**) *Attalea maripa* (AM).

3.2.2. Color Implication of Fresh Fruit and Oil

The orange, yellow–green, and chestnut color of AV, AA, and MF fruits, respectively, are associated with the presence of different levels of carotenoids. Reported values for carotenoids in AV and AA pulps are 8.39 mg/100 g and 6.27 mg/100 g, respectively [81], and 491.05 mg/100 g for MF [82]. The purple color of the OB and EO are associated with high levels of flavonoids including anthocyanins, flavanones, flavanols, and flavones [81–85]. The reported gallic acid equivalence (GAE) for OB is 1759.27 mg 100 g [83,85] and 1880–5890 mg GAE/100 g for EO [83,84]. The color of the fruit is observed in the extracted oil which indicates that these phytochemicals are also present in the oil.

Kernel oil extracted via the cold press method is typically light-yellow or clear while high temperature (>100 °C) methods produce the dark brown colored oil [86]. In this study, the extracted seed oils from the cold-press expeller displayed a transparent light-yellow coloration. This is most likely due to the relatively low extraction temperature used for AAK (50–80 °C), AMK (50–80 °C), AVK (50–80 °C), CGK (37–40 °C), and CNK (31–33 °C) that mitigated oxidative polymerization. It should be noted that many commercial sources of the kernel oils of AV and AA claim that they were cold pressed below 35 °C; however, there is some doubt that this can be accomplished due to the high melting point of these oils and the difficulties associated with controlling temperature at the high pressures required to expel them from the dried kernel [87]. Our group is further researching this concern and will provide further assessments of the volatile components retained in such oils as a function of temperature, including an assessment of the so-called cold pressed and commercially available samples of these oils.

It is also worth noting that cold mechanical press extraction is considered safe and environmentally friendly. Cold pressed oils are generally processed under low temperatures, which minimizes loss beneficial thermolabile volatiles compounds and protects unique flavors and odors [88]. Cold mechanical press extraction yields oils with unique physicochemical characteristics, organoleptic attributes, nutritional quality, oxidative stability, and functional and health-promoting traits [89].

The fresh pulps of AV, AA, OB, and EO are fibrous, oily, and flexible. However, when dried to 5 w/w% moisture content they are brittle and easily breakable. The dried pulps are therefore easier to pulverize than the fresh pulp.

As shown in Figure 7, the kernels of *Oenocarpus bacaba* and *Euterpe oleracea* are different from those of A, AA, AM, and CG in that they have a fibrous network running through the kernel that prevents it from falling out of its shell after drying.

The fresh kernel of AV, AA, EO, AM, CG, and OB cohere strongly to the shell. However, when AV, AA, AM, and CG reach 10–15 w/w% moisture content, the kernel shrinks, detaches, and falls out of the shell. The kernel of fresh CN weakly coheres and can be easily removed from the shell after splitting it. The large kernel seed of MF is easily removed by prying it out; however, they are quite hard and difficult to split and pulverize.

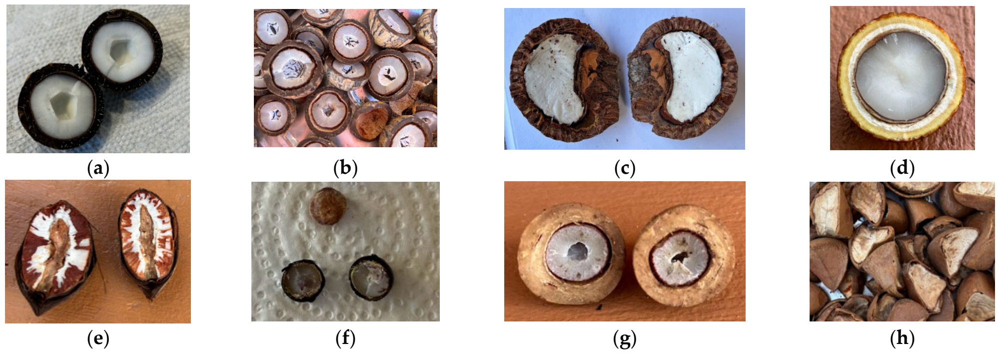

Figure 7. Comparison of split fruit seed kernel. (**a**) Fresh *Astrocaryum aculeatum* (AAK); (**b**) Dried *Astrocaryum aculeatum* (AAK); (**c**) Fresh *Caryocar nuciferum* (CNK); (**d**) Fresh *Mauritia flexuosa* (MFS); (**e**) Fresh *Oenocarpus bacaba* (OBS); (**f**) Fresh *Euterpe oleracea* (EOS); (**g**) Dried *Attalea maripa* (AMS); and (**h**) Fresh *Carapa guianensis* (CGS).

3.3. Mass Balance Data Table for the Eight Tropical Fruits Studied

For each fruit batch studied, a complete mass balance study was performed to account for the distribution of mass throughout the processing stage of the fruits (Table 6). The oil yields for the pulp and/or kernel oils obtained after cold-press extraction are presented in Table 6.

Table 6. Mass balance results of fruit at stages in the drying and oil extraction process. Weight percentages are calculated relative to fresh fruit mass (FFM). Mean percentage and standard deviations are calculated from the combined batches and relative to fresh fruit.

Parameters	AV	AA	OB	EO	MF	CG	CN	AM
Fresh Fruit Mass (FFM) (g)	29,800	12,112	24,000	9500	38,000	14,165	1485	22,700
Fresh Pulp Mass (g)	16,344	5975	6510	2542	20,519	--	--	--
Dried Pulp Mass (g)	11,510	3337	4770	1757	6675	--	--	--
Oil Pulp Mass (g)	2533	1471	682	137	--	--	--	--
Fresh Kernel Mass (g)	12,678	6137	16,843	5848	9130	--	313	22,400
Dried Kernel Mass (g)	6238	4481	--	--	--	8989	173	1632
Deshelled Kernel Mass (g)	5178	1695	--	--	--	5894	--	3904
Kernel Oil Mass (g)	1526	239	--	--	--	2576	45	1632
Pulp Flour Mass (g)	6900	900	3336	1417	--	--	--	--
Kernel Flour Mass (g)	2764	487	--		--	1885	56	1318
Filter Paper Residue Mass (g)	290	-	435	89	--	624	--	747
Fresh pulp moisture (w/w%)	53.5 ± 2.0	29.8 ± 1.1	35.4 ± 1.5	41.2 ± 1.0	71.0 ± 1.1	--	--	--
Dried pulp moisture (w/w%)	5.5 ± 1.0	5.0 ± 1.0	5.0 ± 1.0	5.0 ± 1.1.0	5.9 ± 1.0	--	--	--
Fresh kernel moisture (w/w%)	24.4 ± 2.0	37.2 ± 2.5	--	--	--	50.8 ± 5.2	35.5 ± 1.0	--
Dried kernel moisture (w/w%)	--	--	--	--	--	5.2 ± 1.0	5.0 ± 1.0	4.7 ± 1.0

From Table 6, pulp oil yield was highest for AA (10 w/w%) followed by AV (8 w/w%), OB (3 w/w%), and then EO (1 w/w%). CG kernel oil has the highest oil yield (18 w/w%) followed by AM (7 w/w%), AV (5 ± 1 w/w%), AA (3 w/w%), and then CN (3 w/w%). The estimated standard deviation for pulp and kernel oil yield is ±1 w/w%.

Table 7 compares fruit pulp and/or seed oil yields obtained from cold pressing with the highest optimal oil yields obtained from the literature with common extraction techniques, namely CO_2 supercritical fluid extraction (SFE), Soxhlet extraction, and pressurized fluid extraction (PFE). The oil content is expressed in dry-basis (DB) w/w% (weight of oil/weight of sample × 100%).

From Table 7, AV and AA pulp and kernel oil content were similar using both SFC and cold pressing with an expeller. However, OB and EO oil yield were four times lower from the cold pressing technique compared to SFE. The fibrous nature of both OB and EO pulps posed challenges during extraction which may have contributed to suboptimal yields. Similarly, pulp and seed oil of MF could not be extracted using the cold-pressing expeller as the material clogged in the expeller during the feeding process. CG seed oil content was 2.4 times higher with cold pressing compared to PFE. AM seed oil yield obtained by cold pressing is 23% higher than with Soxhlet extraction with hexane. Typically, Soxhlet and PFE extractions yield higher quantities of oil compared to mechanical cold-pressing [90]. Other factors including ecology, harvest, and processing conditions may play a significant role [91]. In addition, the efficiency of Soxhlet extraction is dependent on the solvent of choice [90]. Hexane is a polar solvent and lacks the ability to extract bound (non-polar) lipids, potentially resulting in reduced yields [92].

Table 7. Comparison of experimental pulp and kernel oils obtained from mechanical cold-pressing extraction with those reported in the literature for extraction using CO_2 supercritical fluid (SFE), Soxhlet extraction with hexane, and pressurized fluid extraction (PFE) with *n*-butane.

Fruit	Literature Oil Content (DB) *w/w*%			Experiment Oil Content (DB) *w/w*%	
	Technique	Pulp	Seed	Pulp	Seed
AV	CO_2 SFE	29.8 *w*/*w*% [93]	17–27 *w*/*w*% [94]	31.5 *w*/*w*%	26.8 *w*/*w*%
AA	CO_2 SFE	33.1 *w*/*w*% [93]	21.9 *w*/*w*% [95]	39.1 *w*/*w*%	18.6 *w*/*w*%
OB	CO_2 SFE	45.3 *w*/*w*% [96]	--	12.7 *w*/*w*%	--
EO	CO_2 SFE	45.4 *w*/*w*% [97]	--	7.8 *w*/*w*%	--
MF	CO_2 SFE	41.1 *w*/*w*% [98]	4.7 *w*/*w*% [99]	--	--
CG	PFE	--	17.8 *w*/*w*% [100]	--	43.7 *w*/*w*%
	Soxhlet	--	61 *w*/*w*% [101]	--	--
AM	Soxhlet	8.9 *w*/*w*% [102]	31.3 *w*/*w*% [102]	--	41.8 *w*/*w*%
CN	--	--	--	--	26 *w*/*w*%

4. Conclusions

The findings of the study will contribute to the design, development, and optimization of ambient drying processes for the fruits studied, pivotal information for local communities, and for the sustainable use of such fruits globally. By leveraging traditional practices like natural drying, one can not only extend the shelf-life of these fruits but also preserve their functional qualities, making them suitable for various applications, including cosmetics and nutraceuticals. This knowledge stands to benefit indigenous communities, support traditional heritage conservation, and enhance the economic potential of tropical fruits and those of palm trees on a global scale.

Supplementary Materials: The following supporting information can be downloaded at https://www.mdpi.com/article/10.3390/pr11123292/s1. Figure S1: (a) Standardized logistic function (SLF) curve fittings of sun-dried AAP, AVP, EOP, OBP and MFP, (b) Standardized logistic function (SLF) curve fittings of shade-dried AAP and AVP, (c) Standardized logistic function (SLF) curve fittings for the sun-dried seeds of AAs and CGS; Figure S2: (a) Modified Page curve fittings of sun-dried AAP, AVP, EOP, OBP and MFP, (b) Modified Page (MP) curve fittings of shade dried AAP and AVP, (c) Modified Page (MP) curve fittings of sun dried AAS and CGS; Figure S3: (a) Lewis model curve fittings of sun-dried AAP, AVP, EOP, OBP and MFP, (b) Standardized logistic function (SLF) curve fittings for the sun-dried seeds of AAs and CGS, (c) Lewis model curve fittings of sun dried AAS and CGS; Table S1: AAP; Table S2: AVP; Table S3: EOP; Table S4: MFP; Table S5: OBP; Table S6: AAP; Table S7: AVP; Table S8: AAS; Table S9: CGS.

Author Contributions: Conceptualization, L.B. and S.S.N.; Methodology, S.D., N.S., L.B. and S.S.N.; Software, S.D., N.S., L.B. and S.S.N.; Validation, S.D., L.B. and S.S.N.; Formal analysis, S.D., N.S., L.B. and S.S.N.; Investigation, S.D., N.S., L.B. and S.S.N.; Resources, S.S.N.; Data curation, S.D., N.S., L.B. and S.S.N.; Writing—original draft, S.D., N.S., L.B. and S.S.N.; Writing—review & editing, S.D., N.S., L.B. and S.S.N.; Visualization, L.B. and S.S.N.; Supervision, N.S., L.B. and S.S.N.; Project administration, S.S.N.; Funding acquisition, S.S.N. All authors have read and agreed to the published version of the manuscript.

Funding: The Sustainable Guyana Program, a partnership between Trent University and the University of Guyana funded by CGX Energy Inc. and Frontera Energy Corporation.

Data Availability Statement: Data is contained within the article or Supplementary Materials.

Conflicts of Interest: The authors declare no conflict of interest.

References

1. Petikirige, J.; Karim, A.; Millar, G. Effect of drying techniques on quality and sensory properties of tropical fruits. *Int. J. Food Sci. Technol.* **2022**, *57*, 6963–6979. [CrossRef]
2. Filho, G.X.d.P.; Ribeiro, A.F.; Moraes, A.F.; Penha, W.F.; Borges, W.L.; Santos, R.H.S. Ethnobotanical Knowledge on Non-conventional Food and Medicinal Plants in Rio Cajari Extractivist Reserve, Amazon, Brazil. *preprint* **2020**. [CrossRef]
3. GBIF Backbone Taxonomy. Checklist Dataset. Available online: https://www.gbif.org/species/7681 (accessed on 15 May 2023).
4. Baker, W.; Dransfield, J. Beyond Genera Palmarum: Progress and prospects in palm systematics. *Bot. J. Linn. Soc.* **2016**, *182*, 207–213. [CrossRef]
5. Yadav, R.; Pednekar, A.; Avalaskar, A.; Rathi, M.; Rewachandani, Y. A comprehensive review on *Meliaceae* family. *World J. Pharm. Sci.* **2015**, *3*, 1572–1577.
6. Prance, G.T.; Da Silva, M.F. Caryocaraceae. *Flora Neotrop.* **1973**, *12*, 1–75.
7. Xu, J.; Wang, X.; Wang, J.; Xu, L.; Zheng, X.; Zhang, Y.; Hu, C. Dominant environmental factors influencing soil metal concentrations of Poyang Lake wetland, China: Soil property, topography, plant species and wetland type. *Catena* **2021**, *207*, 105601. [CrossRef]
8. Guerin, C.; Serret, J.; Montúfar, R.; Vaissayre, V.; Bastos-Siqueira, A.; Durand-Gasselin, T.; Tregear, J.; Morcillo, F.; Dussert, S. Palm seed and fruit lipid composition: Phylogenetic and ecological perspectives. *Ann. Bot.* **2019**, *125*, 157–172. [CrossRef]
9. Teixeira, G.L.; Ibañez, E.; Block, J.M. Emerging Lipids from Arecaceae Palm Fruits in Brazil. *Molecules* **2022**, *27*, 4188. [CrossRef]
10. Koolen, H.H.F.; da Silva, F.M.A.; Gozzo, F.C.; de Souza, A.Q.L.; de Souza, A.D.L. Antioxidant, antimicrobial activities and characterization of phenolic compounds from buriti (*Mauritia flexuosa* L. f.) by UPLC–ESI-MS/MS. *Food Res. Int.* **2013**, *51*, 467–473. [CrossRef]
11. Lescano, C.H.; de Oliveira, I.P.; Freitas de Lima, F.; Baldivia, D.d.S.; Justi, P.N.; Cardoso, C.A.L.; Raposo Júnior, J.L.; Sanjinez-Argandoña, E.J. Nutritional and chemical characterizations of fruits obtained from *Syagrus romanzoffiana*, *Attalea dubia*, *Attalea phalerata* and *Mauritia flexuosa*. *J. Food Meas. Charact.* **2018**, *12*, 1284–1294. [CrossRef]
12. Cordeiro, L.M.C.; de Almeida, C.P.; Iacomini, M. Unusual linear polysaccharides: (1→5)-α-l-Arabinan, (1→3)-(1→4)-α-d-glucan and (1→4)-β-d-xylan from pulp of buriti (*Mauritia flexuosa*), an edible palm fruit from the Amazon region. *Food Chem.* **2015**, *173*, 141–146. [CrossRef]
13. Manhães, L.; Menezes, E.; Marques, A.; Sabaa Srur, A. Flavored Buriti Oil (*Mauritia flexuosa*, Mart.) for Culinary Usage: Innovation, Production and Nutrition Value. *J. Culin. Sci. Technol.* **2015**, *13*, 362–374. [CrossRef]
14. Pereira-Freire, J.A.; Barros, K.B.N.T.; Lima, L.K.F.; Martins, J.M.; Araújo, Y.d.C.; da Silva Oliveira, G.L.; de Souza Aquino, J.; Ferreira, P.M.P. Phytochemistry Profile, Nutritional Properties and Pharmacological Activities of *Mauritia flexuosa*. *J. Food Sci.* **2016**, *81*, R2611–R2622. [CrossRef] [PubMed]
15. Santos, M.D.E.F.G.D.O.S.; Alves, R.E.; Brito, E.S.D.; Silva, S.D.M.; Silveira, M.R.S.D.A. Quality characteristics of fruits and oils of palms native to the Brazilian amazon. *Rev. Bras. Frutic.* **2017**, *39*, e-305. [CrossRef]
16. Silva, A.J.B.d.; Sevalho, E.d.S.; Miranda, I.P.d.A. Potencial das palmeiras nativas da Amazônia Brasileira para a bioeconomia: Análise em rede da produção científica e tecnológica. *Ciência Florest.* **2021**, *31*, 1020–1046. [CrossRef]
17. Rincón-Cervera, M.Á.; Lahlou, A.; Chileh-Chelh, T.; Lyashenko, S.; López-Ruiz, R.; Guil-Guerrero, J.L. Arecaceae Seeds Constitute a Healthy Source of Fatty Acids and Phenolic Compounds. *Plants* **2023**, *12*, 226. [CrossRef] [PubMed]
18. Agostini-Costa, T.D.S. Bioactive compounds and health benefits of some palm species traditionally used in Africa and the Americas—A review. *J. Ethnopharmacol.* **2018**, *224*, 202–229. [CrossRef]
19. Trujillo-Gonzalez, J.M.; Torres Mora, M.A.; Santana-Castañeda, E. La palma de Moriche (*Mauritia flexuosa* Lf;) un ecosistema estratégico. *Orinoquia* **2011**, *15*, 62–70. [CrossRef]
20. James, S.O.; Bouzidi, L.; Emery, R.J.N.; Narine, S.S. Lipid Fractionation and Physicochemical Characterization of Carapa guianensis Seed Oil from Guyana. *Processes* **2023**, *11*, 2565. [CrossRef]
21. Andel, T. *Non-Timber Forest Products of the North-West District of Guyana, Part II (Field Guide)*; Tropenbos-Guyana: Georgetown, Guayana, 2000.

22. Bailão, E.F.L.C.; Devilla, I.A.; Da Conceição, E.C.; Borges, L.L. Bioactive Compounds Found in Brazilian Cerrado Fruits. *Int. J. Mol. Sci.* **2015**, *16*, 23760–23783. [CrossRef]
23. Plowden, C. The ecology and harvest of andiroba seeds for oil production in the Brazilian Amazon. *Conserv. Soc.* **2004**, *2*, 251–272.
24. Dantas, A.R.; Lira-Guedes, A.C.; Mustin, K.; Aparício, W.; Guedes, M.C. Phenology of the multi-use tree species *Carapa guianensis* in a floodplain forest of the Amazon Estuary. *Acta Bot. Bras.* **2016**, *30*, 618–627. [CrossRef]
25. Almeida-Bezerra, J.W.; Bezerra, J.J.L.; Silva, V.B.d.; Coutinho, H.D.M.; Costa, J.G.M.d.; Cruz-Martins, N.; Hano, C.; Menezes, S.A.d.; Morais-Braga, M.F.B.; Oliveira, A.F.M.d. *Caryocar coriaceum* Wittm.(Caryocaraceae): Botany, Ethnomedicinal Uses, Biological Activities, Phytochemistry, Extractivism and Conservation Needs. *Plants* **2022**, *11*, 1685. [CrossRef] [PubMed]
26. Wickens, G.E.; Haq, N.; Day, P.R. *New Crops for Food and Industry*; Springer Science & Business Media: Berlin/Heidelberg, Germany, 1989.
27. Sidhu, J.S.; Zafar, T.A. Super Fruits: Pomegranate, Wolfberry, Aronia (Chokeberry), Acai, Noni, and Amla. In *Handbook of Fruits and Fruit Processing*; Wiley: Hoboken, NJ, USA, 2012; pp. 653–679. [CrossRef]
28. Prance, G.T. The Genus *Caryocar* L. (Caryocaraceae): An Underexploited Tropical Resource. *Adv. Econ. Bot.* **1990**, *8*, 177–188.
29. Ascari, J.; Takahashi, J.; Boaventura, M. The phytochemistry and biological aspects of Caryocaraceae family. *Rev. Bras. Plantas Med.* **2013**, *15*, 293–308. [CrossRef]
30. Lima, A.d.; Silva, A.M.d.O.; Trindade, R.A.; Torres, R.P.; Mancini-Filho, J. Composição química e compostos bioativos presentes na polpa e na amêndoa do pequi (*Caryocar brasiliense*, Camb.). *Rev. Bras. Frutic.* **2007**, *29*, 695–698. [CrossRef]
31. De Araujo, F.D. A Review of *Caryocar brasiliense* (Caryocaraceae): An Economically Valuable Species of the Central Brazilian Cerrados. *Econ. Bot.* **1995**, *49*, 40–48. [CrossRef]
32. Raj, S.P.; Solomon, P.R.; Thangaraj, B.; Raj, S.P.; Solomon, P.R.; Thangaraj, B. Caryocaraceae. In *Biodiesel from Flowering Plants*; Springer: Berlin/Heidelberg, Germany, 2022; pp. 131–134.
33. Sablani, S.S. Drying of Fruits and Vegetables: Retention of Nutritional/Functional Quality. *Dry. Technol.* **2006**, *24*, 123–135. [CrossRef]
34. Roberts, J.S.; Kidd, D.R.; Padilla-Zakour, O. Drying kinetics of grape seeds. *J. Food Eng.* **2008**, *89*, 460–465. [CrossRef]
35. Gokhale, S.B. *Pharmacognosy*; Nirali Prakashan: Pune, India, 2008.
36. Maisnam, D.; Rasane, P.; Dey, A.; Kaur, S.; Sarma, C. Recent advances in conventional drying of foods. *J. Food Technol. Preserv.* **2017**, *1*, 25–34. Available online: http://www.alliedacademies.org/food-technology-and-preservation/ (accessed on 15 May 2023).
37. Mühlbauer, W.; Müller, J. Chapter 2.1-Drying kinetics. In *Drying Atlas*; Mühlbauer, W., Müller, J., Eds.; Woodhead Publishing: Sawstone, UK, 2020; pp. 53–61. [CrossRef]
38. Brennan, J.G. Evaporation and dehydration. In *Food Processing Handbook*; Wiley: Hoboken, NJ, USA, 2006; pp. 71–124.
39. Kahyaoglu, L.N.; Sahin, S.; Sumnu, G. Spouted bed and microwave-assisted spouted bed drying of parboiled wheat. *Food Bioprod. Process.* **2012**, *90*, 301–308. [CrossRef]
40. Falade, K.; Igbeka, J. Osmotic dehydration of tropical fruits and vegetables. *Food Rev. Int.* **2007**, *23*, 373–405. [CrossRef]
41. Silva, M.B.; Perez, V.H.; Pereira, N.R.; Silveira, T.d.C.; da Silva, N.R.F.; de Andrade, C.M.; Sampaio, R.M. Drying kinetic of tucum fruits (*Astrocaryum aculeatum* Meyer): Physicochemical and functional properties characterization. *J. Food Sci. Technol.* **2018**, *55*, 1656–1666. [CrossRef] [PubMed]
42. da Silva, R.S.; Aguiar, N.V.; Durigon, A.; de Oliveira, A.M., Jr. Cast-tape drying and freeze drying of tucumã pulp into powder. *J. Food Process Eng.* **2022**, *45*, e13956. [CrossRef]
43. Pereira, C.B.; de Souza, J.B.; da Costa Santos, D.; de Farias Leite, D.D.; de Lima Ferreira, J.P.; de Oliveira, E.N.A. Modelagem e propriedades termodinâmicas da secagem do epicarpo, mesocarpo e endocarpo do tucumã (*Astrocaryum aculeatum*). *Braz. J. Food Technol.* **2022**, *1*, 1–18. [CrossRef]
44. Oliveira, N.L.; Silva, S.H.; Figueiredo, J.d.A.; Norcino, L.B.; Resende, J.V.d. Infrared-assisted freeze-drying (IRFD) of açai puree: Effects on the drying kinetics, microstructure and bioactive compounds. *Innov. Food Sci. Emerg. Technol.* **2021**, *74*, 102843. [CrossRef]
45. Simão, R.d.S.; Zhang, L.; Moraes, J.O.d.; Schröder, A.; Laurindo, J.B.; Schutyser, M.A.I. Low-pressure conductive thin film drying of açaí pulp. *LWT* **2022**, *164*, 113695. [CrossRef]
46. Nagata, G.A.; Costa, T.V.; Perazzini, M.T.B.; Perazzini, H. Coupled heat and mass transfer modelling in convective drying of biomass at particle-level: Model validation with experimental data. *Renew. Energy* **2020**, *149*, 1290–1299. [CrossRef]
47. Morais, M.F.d.; dos Santos, J.R.; Santos, M.P.d.; Santos, D.d.C.; Costa, T.N.d.; Lima, J.B. Modeling and thermodynamic properties of 'bacaba' pulp drying. *Rev. Bras. Eng. Agrícola Ambient.* **2019**, *23*, 702–708. [CrossRef]
48. Resende, L.M.; Franca, A.S.; Oliveira, L.S. Buriti (*Mauritia flexuosa* L. f.) fruit by-products flours: Evaluation as source of dietary fibers and natural antioxidants. *Food Chem.* **2019**, *270*, 53–60. [CrossRef]
49. Chen, C.; Pan, Z. An overview of progress, challenges, needs and trends in mathematical modeling approaches in food drying. *Dry. Technol.* **2023**, 1–20. [CrossRef]
50. Akter, F.; Muhury, R.; Sultana, A.; Deb, U.K. A Comprehensive Review of Mathematical Modeling for Drying Processes of Fruits and Vegetables. *Int. J. Food Sci.* **2022**, *2022*, 6195257. [CrossRef] [PubMed]
51. Buzrul, S. Reassessment of Thin-Layer Drying Models for Foods: A Critical Short Communication. *Processes* **2022**, *10*, 118. [CrossRef]

52. Lewis, W.K. The Rate of Drying of Solid Materials. *J. Ind. Eng. Chem.* **1921**, *13*, 427–432. [CrossRef]
53. Hutchinson, D.; Otten, L. Thin-layer air drying of soybeans and white beans. *Int. J. Food Sci. Technol.* **1983**, *18*, 507–522. [CrossRef]
54. Alibas, I. Microwave, air and combined microwave–air-drying parameters of pumpkin slices. *LWT-Food Sci. Technol.* **2007**, *40*, 1445–1451. [CrossRef]
55. Page, G.E. *Factors Influencing the Maximum Rates of Air Drying Shelled Corn in Thin Layers*; Purdue University: West Lafayette, IN, USA, 1949.
56. Overhults, D.G.; White, G.; Hamilton, H.; Ross, I. Drying soybeans with heated air. *Trans. ASAE* **1973**, *16*, 112–113. [CrossRef]
57. Corzo, O.; Bracho, N.; Pereira, A.; Vásquez, A. Weibull distribution for modeling air drying of coroba slices. *LWT-Food Sci. Technol.* **2008**, *41*, 2023–2028. [CrossRef]
58. Karacabey, E.; Buzrul, S. Modeling and predicting the drying kinetics of apple and pear: Application of the Weibull model. *Chem. Eng. Commun.* **2017**, *204*, 573–579. [CrossRef]
59. Johnson, M. Parameter correlations while curve fitting. *Methods Enzymol.* **2000**, *321*, 424–446. [CrossRef]
60. Whitaker, S. Simultaneous Heat, Mass, and Momentum Transfer in Porous Media: A Theory of Drying. In *Advances in Heat Transfer*; Hartnett, J.P., Irvine, T.F., Eds.; Elsevier: Amsterdam, The Netherlands, 1977; Volume 13, pp. 119–203.
61. Erbay, Z.; Icier, F. A Review of Thin Layer Drying of Foods: Theory, Modeling, and Experimental Results. *Crit. Rev. Food Sci. Nutr.* **2010**, *50*, 441–464. [CrossRef] [PubMed]
62. The-Weather-Channel. Weather in Georgetown, Demerara-Mahaica, Guyana. USA. 2023. Available online: https://weather.com/weather/today/l/6.80,-58.15?par=google (accessed on 17 September 2023).
63. Mujumdar, A.S. *Handbook of Industrial Drying*; CRC Press: Boca Raton, FL, USA, 2006.
64. Henderson, S. Grain drying theory, I. Temperature effect on drying coefficient-No Paper Link Available. *J. Agr. Eng. Res.* **1961**, *6*, 169–173.
65. Tsoularis, A.; Wallace, J. Analysis of logistic growth models. *Math. Biosci.* **2002**, *179*, 21–55. [CrossRef]
66. Burgos-Simón, C.; Cortés, J.-C.; Martínez-Rodríguez, D.; Villanueva, R.J. Modeling breast tumor growth by a randomized logistic model: A computational approach to treat uncertainties via probability densities. *Eur. Phys. J. Plus* **2020**, *135*, 826. [CrossRef]
67. Yin, X.; Zelenay, P. (Invited) Kinetic Models for the Degradation Mechanisms of PGM-Free ORR Catalysts. *ECS Trans.* **2018**, *85*, 1239. [CrossRef]
68. Pelinovsky, E.; Kurkin, A.; Kurkina, O.; Kokoulina, M.; Epifanova, A. Logistic equation and COVID-19. *Chaos Solitons Fractals* **2020**, *140*, 110241. [CrossRef]
69. Reed, L.J.; Berkson, J. The Application of the Logistic Function to Experimental Data. *J. Phys. Chem.* **1929**, *33*, 760–779. [CrossRef]
70. Cunha, L.M.; Oliveira, F.A.R.; Oliveira, J.C. Optimal experimental design for estimating the kinetic parameters of processes described by the Weibull probability distribution function. *J. Food Eng.* **1998**, *37*, 175–191. [CrossRef]
71. Motulsky, H.; Christopoulos, A. *Fitting Models to Biological Data Using Linear and Nonlinear Regression: A Practical Guide to Curve Fitting*; Oxford University Press: Oxford, UK, 2004.
72. Van Boekel, M. To pool or not to pool: That is the question in microbial kinetics. *Int. J. Food Microbiol.* **2021**, *354*, 109283. [CrossRef]
73. Zelinka, S.L.; Kirker, G.T.; Bishell, A.B.; Glass, S.V. Effects of Wood Moisture Content and the Level of Acetylation on Brown Rot Decay. *Forests* **2020**, *11*, 299. [CrossRef]
74. Barrett, J.P. The Coefficient of Determination—Some Limitations. *Am. Stat.* **1974**, *28*, 19–20. [CrossRef]
75. Cunha, L.M.; Oliveira, F.A.; Aboim, A.P.; Frías, J.M.; Pinheiro-Torres, A. Stochastic approach to the modelling of water losses during osmotic dehydration and improved parameter estimation. *Int. J. Food Sci. Technol.* **2001**, *36*, 253–262. [CrossRef]
76. Surendhar, A.; Sivasubramanian, V.; Vidhyeswari, D.; Deepanraj, B. Energy and exergy analysis, drying kinetics, modeling and quality parameters of microwave-dried turmeric slices. *J. Therm. Anal. Calorim.* **2019**, *136*, 185–197. [CrossRef]
77. Motevali, A.; Minaei, S.; Banakar, A.; Ghobadian, B.; Darvishi, H. Energy analyses and drying kinetics of chamomile leaves in microwave-convective dryer. *J. Saudi Soc. Agric. Sci.* **2016**, *15*, 179–187. [CrossRef]
78. Soysal, Y.; Öztekin, S.; Eren, Ö. Microwave drying of parsley: Modelling, kinetics, and energy aspects. *Biosyst. Eng.* **2006**, *93*, 403–413. [CrossRef]
79. Darvishi, H.; Asl, A.R.; Asghari, A.; Azadbakht, M.; Najafi, G.; Khodaei, J. Study of the drying kinetics of pepper. *J. Saudi Soc. Agric. Sci.* **2014**, *13*, 130–138. [CrossRef]
80. Zarein, M.; Samadi, S.H.; Ghobadian, B. Investigation of microwave dryer effect on energy efficiency during drying of apple slices. *J. Saudi Soc. Agric. Sci.* **2015**, *14*, 41–47. [CrossRef]
81. Noronha Matos, K.A.; Praia Lima, D.; Pereira Barbosa, A.P.; Zerlotti Mercadante, A.; Campos Chisté, R. Peels of tucumã (*Astrocaryum vulgare*) and peach palm (*Bactris gasipaes*) are by-products classified as very high carotenoid sources. *Food Chem.* **2019**, *272*, 216–221. [CrossRef]
82. do Nascimento Silva, N.R.R.; Cavalcante, R.B.M.; da Silva, F.A. Nutritional properties of Buriti (*Mauritia flexuosa*) and health benefits. *J. Food Compos. Anal.* **2023**, *117*, 105092. [CrossRef]
83. Finco, F.; Kammerer, D.R.; Carle, R.; Tseng, W.-H.; Böser, S.; Graeve, L. Antioxidant activity and characterization of phenolic compounds from bacaba (*Oenocarpus bacaba* Mart.) fruit by HPLC-DAD-MS. *J. Agric. Food Chem.* **2012**, *60*, 7665–7673. [CrossRef] [PubMed]

84. Xiong, J.; Matta, F.V.; Grace, M.; Lila, M.A.; Ward, N.I.; Felipe-Sotelo, M.; Esposito, D. Phenolic content, anti-inflammatory properties, and dermal wound repair properties of industrially processed and non-processed acai from the Brazilian Amazon. *Food Funct.* **2020**, *11*, 4903–4914. [CrossRef] [PubMed]
85. Kang, J.; Xie, C.; Li, Z.; Nagarajan, S.; Schauss, A.G.; Wu, T.; Wu, X. Flavonoids from acai (*Euterpe oleracea* Mart.) pulp and their antioxidant and anti-inflammatory activities. *Food.Chem* **2011**, *128*, 152–157. [CrossRef] [PubMed]
86. Chen, X.; Sun, S. Color Reversion of Refined Vegetable Oils: A Review. *Molecules* **2023**, *28*, 5177. [CrossRef] [PubMed]
87. Gomes, A.T.A.; Pereira, R.R.; Duarte Junior, A.P.; da Cruz Rodrigues, A.M.; Remédios, C.M.R.; Brasil, D.d.S.B.; Morais, L.R.B.; Silva-Júnior, J.O.C.; Ribeiro-Costa, R.M. Tucumã (*Astrocaryum vulgare*) fat: An Amazonian material as a pharmaceutical input for lipid nanoparticle production. *J. Therm. Anal. Calorim.* **2020**, *147*, 355–365. [CrossRef]
88. Zhang, W.; Cao, X.; Liu, S.Q. Aroma modulation of vegetable oils—A review. *Crit. Rev. Food Sci. Nutr.* **2020**, *60*, 1538–1551. [CrossRef] [PubMed]
89. Ramadan, M.F. (Ed.) Chapter 1-Introduction to cold pressed oils: Green technology, bioactive compounds, functionality, and applications. In *Cold Pressed Oils*; Academic Press: Cambridge, MA, USA, 2020; pp. 1–5. [CrossRef]
90. Danlami, J.M.; Arsad, A.; Ahmad Zaini, M.A.; Sulaiman, H. A comparative study of various oil extraction techniques from plants. *Rev. Chem. Eng.* **2014**, *30*, 605–626. [CrossRef]
91. Mehalaine, S.; Chenchouni, H. Quantifying how climatic factors influence essential oil yield in wild-growing plants. *Arab. J. Geosci.* **2021**, *14*, 1257. [CrossRef]
92. Fornasari, C.H.; Secco, D.; Santos, R.F.; da Silva, T.R.B.; Lenz, N.B.G.; Tokura, L.K.; Lenz, M.L.; Souza, S.N.M.d.; Junior, L.A.Z.; Gurgacz, F. Efficiency of the use of solvents in vegetable oil extraction at oleaginous crops. *Renew. Sustain. Energy Rev.* **2017**, *80*, 121–124. [CrossRef]
93. Costa, B.E.T.; Santos, O.V.d.; CorrÊA, N.C.F.; FranÇA, L.F.d. Comparative study on the quality of oil extracted from two tucumã varieties using supercritical carbon dioxide. *Food Sci. Technol.* **2016**, *36*, 322–328. [CrossRef]
94. Didonet, A.A.; Antoniassi, R.; Back, G.R.; de Faria-Machado, A.F.; Wilhelm, A.E.; Ferraz, I.D.K. Characterization of Amount and Quality of Tucuman Kernel Oil as a Potential Biomass. *J. Am. Oil Chem. Soc.* **2020**, *97*, 955–962. [CrossRef]
95. Zaninetti, R.; Moreira, A.; Ferraudo, A.; Teixeira, S. Population variability in production of oil, total lipids in kernel and pulp of tucumã (*Astrocaryum aculeatum*) collected in the Acre State, Brazil. *Agrotrópica* **2016**, *28*, 179–184. [CrossRef]
96. Cunha, V.M.B.; Silva, M.P.d.; Sousa, S.H.B.d.; Bezerra, P.d.N.; Menezes, E.G.O.; Silva, N.J.N.d.; Banna, D.A.D.d.S.; Araújo, M.E.; Carvalho Junior, R.N.d. Bacaba-de-leque (*Oenocarpus distichus* Mart.) oil extraction using supercritical CO_2 and bioactive compounds determination in the residual pulp. *J. Supercrit. Fluids* **2019**, *144*, 81–90. [CrossRef]
97. de Cássia Rodrigues Batista, C.; de Oliveira, M.S.; Araújo, M.E.; Rodrigues, A.M.C.; Botelho, J.R.S.; da Silva Souza Filho, A.P.; Machado, N.T.; Carvalho, R.N. Supercritical CO_2 extraction of açaí (*Euterpe oleracea*) berry oil: Global yield, fatty acids, allelopathic activities, and determination of phenolic and anthocyanins total compounds in the residual pulp. *J. Supercrit. Fluids* **2016**, *107*, 364–369. [CrossRef]
98. Best, I.; Cartagena-Gonzales, Z.; Arana-Copa, O.; Olivera-Montenegro, L.; Zabot, G. Production of Oil and Phenolic-Rich Extracts from *Mauritia flexuosa* L.f. Using Sequential Supercritical and Conventional Solvent Extraction: Experimental and Economic Evaluation. *Processes* **2022**, *10*, 459. [CrossRef]
99. Balick, M.J. Amazonian oil palms of promise: A survey. *Econ. Bot.* **1979**, *33*, 11–28. [CrossRef]
100. Novello, Z.; Scapinello, J.; Magro, J.D.; Zin, G.; Luccio, M.D.; Tres, M.V.; Oliveira, J.V. Extraction, chemical characterization and antioxidant activity of andiroba seeds oil obtained from pressurized n-butane. *Ind. Crops Prod.* **2015**, *76*, 697–701. [CrossRef]
101. Araujo-Lima, C.F.; Fernandes, A.S.; Gomes, E.M.; Oliveira, L.L.; Macedo, A.F.; Antoniassi, R.; Wilhelm, A.E.; Aiub, C.A.F.; Felzenszwalb, I. Antioxidant Activity and Genotoxic Assessment of Crabwood (Andiroba, *Carapa guianensis* Aublet) Seed Oils. *Oxidative Med. Cell. Longev.* **2018**, *2018*, 3246719. [CrossRef] [PubMed]
102. Bereau, D.; Benjelloun-Mlayah, B.; Delmas, M. Maximiliana maripa drude mesocarp and kernel oils: Fatty acid and total tocopherol compositions. *J. Am. Oil Chem. Soc.* **2001**, *78*, 213–214. [CrossRef]